Chalcogenide Letters Vol. 19, No. 11, November 2022, p. 793 - 803

First-principles calculations of the dynamical and thermodynamic properties of lead chalcogenides PbX (X = S, Se, Te)

Y. Yu*, X. G. Kong, Y. H. Shen, G. Q. Yin
College of Optoelectronic Engineering, Chengdu University of Information Technology, Chengdu 610225, China

We perform first-principles calculations of the dynamical and thermodynamic properties of lead chalcogenides PbX (X = S, Se, Te). Using density functional perturbation theory, we obtain the phonon frequencies and the phonon dispersion curves, as well as corresponding density of states. The calculated phonon frequencies at the Γ, X, and L points of the Brillouin zone show good agreement with the experimental values for most vibration modes. The thermodynamics properties including the phonon contribution to the Helmholtz free energy ΔF, the phonon contribution to the internal energy ΔE, the entropy S, and the constant-volume specific heat C_v are determined within the harmonic approximation based on the calculated phonon dispersion relations. The difference values of H-H_{298} have been also calculated and compared with the available experimental data.

(Received August 21, 2022; Accepted November 4, 2022)

Keywords: Lead chalcogenides, DFPT, Dynamical, Thermodynamic

1. Introduction

Lead chalcogenides PbX (X = S, Se, Te), a family of narrow band gap IV-VI semiconductors, have been the subject of intensive research due to their applications in many fields such as thermoelectric converters [1-3], infrared lasers [4], light-emitting diodes [5], window coatings [6] and solar-energy panels [7]. They have also attracted significant theoretical interest aimed at understanding the physics of their phase transitions, electronic band gaps, and ferroelectric-like behavior at low temperatures. As narrow gap semiconductor compounds, lead chalcogenides exhibit outstanding optical and electrical transport properties. Moreover, they exhibit low thermal conductivities at high temperatures, which is unusual for simple structured materials. For a long time, their unique electronic properties and heat transport characteristics have made them the focus of thermoelectric materials research.

There have been many high-quality *ab initio* calculations of the electronic properties of PbX (X = Te, Se, S) [8-10]. Most of the research works were focused on electronic band structures modification and electron transport properties. Nevertheless, there are only few studies on lattice dynamics and thermodynamic properties. The thermodynamic properties are one of the most basic properties of any material and depend on the lattice dynamical behaviour. Experimentally, the phonon dispersion relations of PbS, PbSe, and PbTe, which reflect their simple rocksalt-type

* Corresponding author: yy2012@cuit.edu.cn
https://doi.org/10.15251/CL.2022.1911.793

crystal structure, have been investigated at room temperature by means of inelastic neutron scattering (INS) [11-13]. On the theoretical side, there have been a few studies to calculate the lattice dynamics and thermodynamic properties by first-principles methods [14-19].

The main aim of this work is to provide a thorough density functional perturbation theory (DFPT) [20,21] investigation of the thermodynamic properties of PbX at 0 K and high temperature. Since lattice vibration constitutes main contribution to thermodynamic function of materials at finite temperatures, detailed information on the phonon spectrum is crucial for understanding the thermodynamic properties under finite temperatures. The phonon density of states (DOS), which includes contributions from all phonon over the entire Brillouin zone, is needed for the calculations of various thermodynamic functions under the harmonic approximation [22,23], e.g. the phonon contribution to the Helmholtz free energy ΔF, the phonon contribution to the internal energy ΔE, the entropy S, and the constant-volume specific heat C_v.

2. Computational methods

The dynamical and thermodynamic properties of PbX (X = S, Se, Te) compounds in rocksalt-type cubic structures are investigated from first-principles calculations based on density functional theory (DFT) [24,25] using projector augmented waves (PAW) [26] potentials within the local density approximation (LDA) for modeling exchange-correlation effects. The calculations are performed using the ABINIT package [27,28], which is based on pseudopotentials and plane waves. The wave functions are expanded in plane waves up to a kinetic energy cutoff of 30 hartree. Integrals over the Brillouin zone (BZ) are replaced by a sum on a Monkhorst-pack grid of 6×6×6 special ***k***-point. Convergence tests show that the BZ sampling and the kinetic energy cutoff are sufficient to guarantee an excellent convergence within 1 cm^{-1} for the calculated phonon frequencies.

Phonon dispersion curves were obtained using the first principles linear response theory [29] of the density functional perturbation theory (DFPT), which avoids the used of supercells and allows the calculation of the dynamical matrix at arbitrary q vectors. The thermodynamic functions of PbX can be determined by the phonon frequencies and phonon densities of state.

3. Results and discussion

3.1. Structural properties

The rocksalt-type structure PbX (X = S, Se, Te) has a cubic symmetry and belongs to the space group Fm-3m. The primitive cell consists of two atoms. The Pb atom is located in the 4*b* Wyckoff site (0.5, 0.5, 0.5) and the X atom occupies the 4*a* (0, 0, 0) site. We first determine the equilibrium volume of the ground state of PbX by calculating the total energy per primitive unit cell as a function of volume. Because these compounds have very high symmetry, we have only optimized the volume keeping the angles fixed and not optimized the atomic position. The spin-orbit (*s-o*) interaction was found to change the lattice constant by ~0.1% in these materials [17], so *s-o* interaction was not taken into account in structural optimization.

Table 1 displays the obtained lattice parameters compared to other calculations and experimental data reported in the literature. The optimised lattice constant *a* is 5.848 Å for PbS, 6.043 Å for PbSe and 6.379 Å for PbTe, which are very near to the experimental values of 5.929, 6.117 and 6.443Å, respectively. Our calculations overestimate the equilibrium lattice parameter with the maximal error of 1.39% with respect to experimental values, a normal agreement by LDA standards. Considering that the zero-point motion and thermal effects are not taken into account, the calculated lattice constants agree quite well with the experimental ones. This is largely sufficient to allow the further study of dynamical and thermodynamic properties.

Table 1 Calculated and experimental lattice parameters a (in Å) for PbX (X = S, Se, Te).

		a (Å)				
		Present		Calc.		Expt.
PbS		5.848		5.842[17], 5.810[18], 6.007[19], 5.906[30]		5.936[31], 5.929[32]
PbSe		6.043		6.012[17], 6.039[18], 6.212[19], 6.098[30]		6.124 [31], 6.117[32]
PbTe		6.379		6.318[17], 6.382[18], 6.562[19], 6.439[30]		6.462[31], 6.443[32]

3.2. Dynamical properties

PbX (X = S, Se, Te) semiconductors belong to the cubic system, with point group O_h and space group Fm-3m. According to lattice vibration theory [33], vibration frequency ω is a function of wave vector q, which is described with the dispersion relation: $\omega = \omega_j(q)$. The subscript j is the branch index. A crystal lattice with n atoms per unit cell has $3n$ branches, three of which are acoustic and the remainder optical. There are 2 atoms in the primitive unit cell of PbX crystal, so there are 6 dispersion curves, which mean 6 normal vibration modes at the center Γ point. Based on the factor group theory, the reducible representations for the space group Fm-3m at the Γ point can be reduced as follows:

Wyckoff Position 4*a*: T_{1u};
Wyckoff Position 4*b*: T_{1u}.

The irreducible representations of the lattice vibration in PbX are the following: $2T_{1u}$. Grouptheoretical analysis predicts the following irreducible representation for acoustical and optical zone center modes: $\Gamma_{aco}=T_{1u}$ and $\Gamma_{opt}=T_{1u}$. T_{1u} symmetry mode is triply degenerate, and is not Raman active but infrared active. In particular, the dipole-dipole contribution is found to be responsible for the splitting between the longitudinal and transverse optic (LO and TO, respectively) modes T_{1u}.

The spin-orbit interaction was not treated in our phonon calculations since the related calculations are very time consuming, and the work in Ref. [16] suggests that it has a minimal effect on lattice vibrations. The results for the phonon dispersion curves of PbX along several high-symmetry lines together with the corresponding phonon density of states (DOS) are displayed

in Fig. 1-3. The phonon DOS is normalized to the number of phonons with $\int_0^\infty g(\omega)d\omega = 1$. The mass of Pb atoms is much larger than that of S, Se, and Te, so the acoustic branches correspond almost exclusively to vibrations of lead ions. Thus, the acoustic mode dispersion is quantitatively very similar in the three lead chalcogenides. The main difference is that the frequency decreases somewhat as the lattice constant increases in the series PbS, PbSe, and PbTe. The three optical branches correspond to the vibrations of the anions. There is a vanishing energy gap between acoustic and optical modes for the three lead chalcogenides, showing a continuous DOS, which is in agreement with Ref. [16-19].

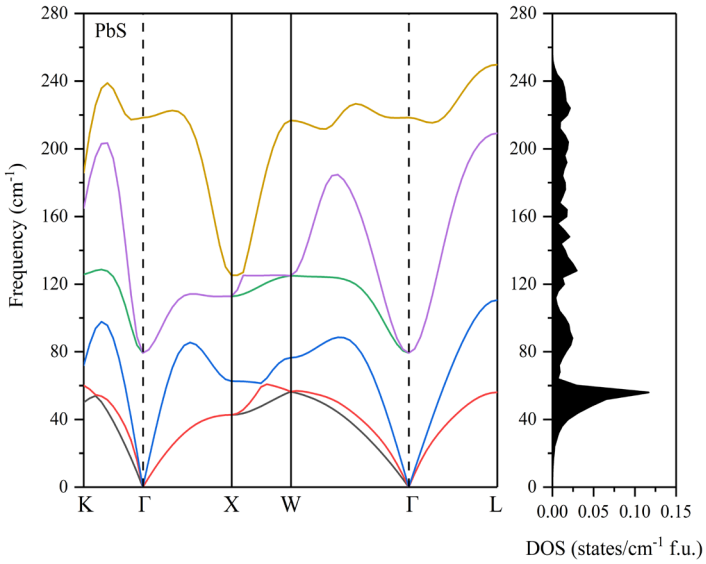

Fig. 1. Calculated phonon dispersion curves along high-symmetry lines in the Brillouin zone and the corresponding phonon density of states (DOS) for PbS.

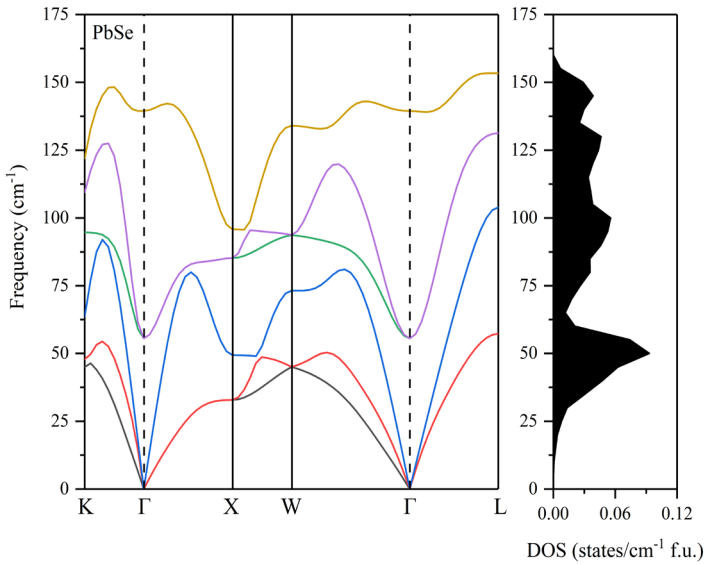

Fig. 2. Calculated phonon dispersion curves along high-symmetry lines in the Brillouin zone and the corresponding phonon density of states (DOS) for PbSe.

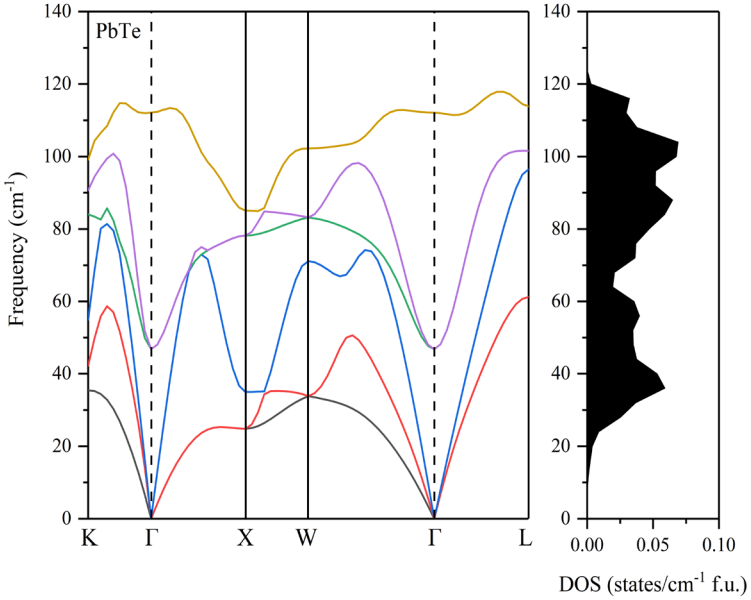

Fig. 3. Calculated phonon dispersion curves along high-symmetry lines in the Brillouin zone and the corresponding phonon density of states (DOS) for PbTe.

The results for the phonon frequencies along several high-symmetry points (at Γ, X, and L points) of PbX are compared with the experimental values and other calculations in Table 2. The calculated values are found to be in excellent agreement with experimental data[11,12,13] and other calculations[17]. The splittings occur remarkably between T_{1u}(LO) and T_{1u}(TO) at Γ point due to the generally large calculated Born effective charge. On the other hand, large Born effective charge suggests that the PbX (X = S, Se, Te) can be strongly polarized with atomic displacements. The LO/TO splitting at the zone-centre corresponds to 139.1, 83.8 and 65.3 cm^{-1} for PbS, PbSe, and PbTe, respectively. This splitting, particularly for PbS, is stronger than the other two compounds. PbS has higher optical phonon branches in frequency than PbTe and PbSe, which is due to the largest mass difference between Pb and S.

Table 2. Phonon frequencies (in cm^{-1}) at certain high-symmetry point (Γ, X, and L points) in the Brillouin zone of PbX (X= S, Se, Te).

Compound		Γ (0, 0, 0)			X (0.5, 0, 0.5)					L (0.5, 0.5, 0.5)			
		LO	TO		LO	TO	LA	TA		LO	TO	LA	TA
PbS	Present	218.4	79.3		125.3	112.9	62.6	42.7		249.8	209.2	110.6	56.0
	Calc.[17]	210.5	63.7		113.7	96.7	53.4	39.7		243.5	193.5	108.1	51.0
	Expt.[11]	223.5	65.0		92.4	88.4	54.7	40.0		237.8	194.1	101.7	49.4
PbSe	Present	139.4	55.6		95.8	85.2	49.4	32.9		153.3	131.3	103.9	57.3
	Calc.[17]	143.1	47.7		86.1	74.4	47.7	33.7		149.1	122.8	102.4	54.4
	Expt.[13]	133.1	43.7										
PbTe	Present	112.1	46.8		85.1	78.2	35.0	24.8		113.8	101.6	96.5	61.2
	Calc.[17]	114.1	34.7		73.7	64.4	33.0	24.2		108.1	93.4	93.1	55.4
	Expt.[12]	114.1	31.7		78.4	69.4	32.7	24.0		95.4	90.7	91.4	54.4

3.3. Thermodynamic properties

The knowledge of the entire phonon spectrum granted by DFPT makes possible the calculation of several important thermodynamical properties as functions of temperature T. In the present work, the phonon contribution to the Helmholtz free energy ΔF, the phonon contribution to the internal energy ΔE, the entropy S, and the constant-volume specific heat C_v, at temperature T, are calculated using the formulas in Ref. [34] within the harmonic approximation:

$$\Delta F = 3nNk_BT\int_0^{\omega_{\max}} \ln\left\{2\sinh\frac{\hbar\omega}{2k_BT}\right\}g(\omega)d\omega \tag{1}$$

$$\Delta E = 3nN\frac{\hbar}{2}\int_0^{\omega_{\max}} \omega\coth\left(\frac{\hbar\omega}{2k_BT}\right)g(\omega)d\omega \tag{2}$$

$$S = 3nNk_B\int_0^{\omega_{\max}}\left[\frac{\hbar\omega}{2k_BT}\coth\frac{\hbar\omega}{2k_BT} - \ln\left\{2\sinh\frac{\hbar\omega}{2k_BT}\right\}\right]\times g(\omega)d\omega \tag{3}$$

$$C_v = 3nNk_B\int_0^{\omega_{\max}}\left(\frac{\hbar\omega}{2k_BT}\right)^2 \operatorname{csc}h^2\left(\frac{\hbar\omega}{2k_BT}\right)g(\omega)d\omega \tag{4}$$

where k_B is the Boltzman constant, n is the number of atoms per unit cell, N is the number of unit cells, ω is the phonon frequencies, $\omega_{\max}$ is the largest phonon frequency, and $g(\omega)$ is the normalized phonon density of states with $\int_0^{\omega_{\max}} g(\omega)d\omega = 1$. In Fig. 4 and 5, we have displayed the relations of the ΔF and ΔE as a function of the temperature T from 0 to 1200K. ΔF and ΔE at zero temperature represent the zero-point motion, which can be calculated from the expression as $\Delta F_0 = \Delta E_0 = 3nN\int_0^{\omega_{\max}} (\hbar\omega/2)g(\omega)d\omega$. For PbS, the calculated ΔF_0 = ΔE_0 = 4.2 KJ/mol. In addition, the value is 3.0 for PbSe, and 2.6 for PbTe. The zero-point motion contribution to the thermodynamic functions ΔF and ΔE of PbS is more prominent since PbS has much higher average phonon frequencies.

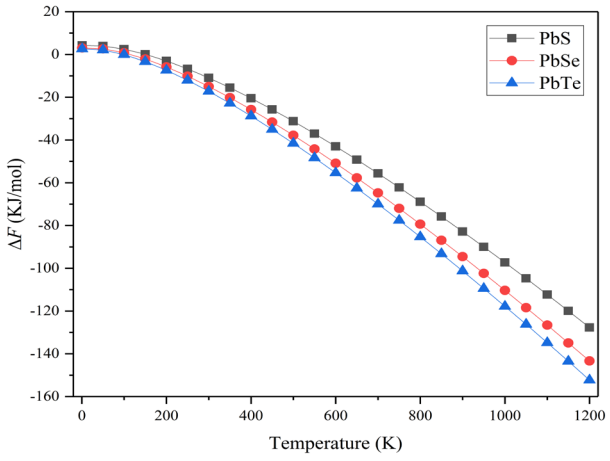

Fig. 4. The phonon contribution to the Helmholtz free energies ΔF of PbX (X = S, Se, Te).

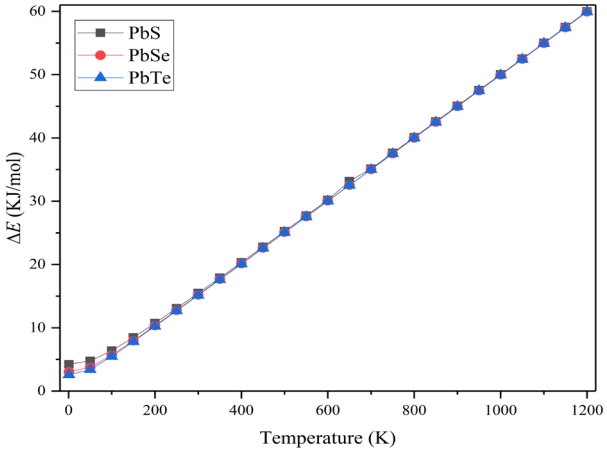

Fig. 5. The phonon contribution to the internal energies ΔE of PbX (X = S, Se, Te).

The calculated constant-volume heat capacity C_v of PbX as a function of T is shown in Fig. 6. PbS is found to have lower C_v than the other two compounds over the entire temperature range, due to its phonon density of states for low-frequency modes. In the high temperature, all three curves display the typical convergence toward the Dulong and Petit value $6N_Ak_B = 49.9$ J/mol K for a material with two atoms in the primitive cell.

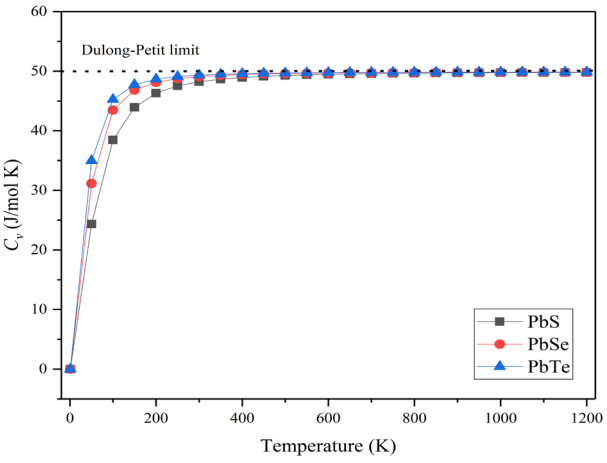

Fig. 6. The constant-volume specific heats of PbX (X = S, Se, Te).

Entropy S and enthalpy H are two important physical quantities in thermodynamics. The enthalpy can be written as:

$$H = E + \Delta E + pV. \tag{5}$$

where E is the static contribution to the internal energy. For a simple system, with a constant number of particles, the difference in enthalpy is the maximum amount of thermal energy derivable from a thermodynamic process with a constant pressure. If 298 K is taken as a reference

temperature, the difference values of $H\text{-}H_{298}$ can be calculated with the interval 100 K. The calculated results S and $H\text{-}H_{298}$ are displayed in Tables 3-5 together with the corresponding experimental data [35]. The calculated results exhibit reasonable agreement with the experimental values. The variations of entropy S with temperature exhibits a similar trend for all lead chalcogenides. We notice that the entropy decreases when the size of the anion atoms (X) decrease. For low temperatures, our harmonic approximation works best, and the calculated values of S and $H\text{-}H_{298}$ can be compared to the experimental value. The larger error at higher temperature may suggest the limitation of the quasiharmonic approximation, because the quasiharmonic approximation accounts only partially for the effects of anharmonicity. Another cause of errors may be the effect of the electron-phonon interaction in PbX system, which is not included in our calculations.

Table 3. The comparison between the calculated and experimental S and $H\text{-}H_{298}$ of PbS.

T (K)	Calculated results			Experimental results[35]	
	S (J/mol K)	($H\text{-}H_{298}$) (KJ/mol)		S (J/mol K)	($H\text{-}H_{298}$) (KJ/mol)
298.15	87.751	0.000		91.343	0.000
300	88.073	0.096		91.649	0.091
400	102.058	4.959		106.016	5.088
500	113.018	9.872		117.383	10.184
600	122.020	14.809		126.847	15.376
700	129.653	19.761		134.996	20.664
800	136.278	24.722		142.183	26.047
900	142.128	29.689		148.634	31.525
1000	147.366	34.661		154.504	37.097
1100	152.107	39.611		159.905	42.764
1200	156.438	44.587		164.917	48.526
1300	160.422	49.566		169.604	54.382
1386.5	163.613	53.874		173.433	59.524

Table 4. The comparison between the calculated and experimental S and $H\text{-}H_{298}$ of PbSe.

T (K)	Calculated results			Experimental results[35]	
	S (J/mol K)	($H\text{-}H_{298}$) (KJ/mol)		S (J/mol K)	($H\text{-}H_{298}$) (KJ/mol)
298.15	100.288	0.000		102.508	0.000
300	100.616	0.098		102.819	0.093
400	114.792	5.027		117.408	5.167
500	125.842	9.979		128.949	10.340
600	134.893	14.943		138.561	15.614
700	142.557	19.915		146.843	20.988
800	149.201	24.890		154.150	26.462
900	155.064	29.869		160.714	32.035
1000	160.312	34.850		166.691	37.709
1100	165.060	39.832		172.193	43.483
1200	169.386	44.815		177.303	49.356
1300	173.386	49.799		182.084	55.330
1359	175.598	52.740		184.771	58.901

Table 5. The comparison between the calculated and experimental S and H-H_{298} of PbTe.

T (K)	Calculated results			Experimental results[35]	
	S (J/mol K)	(H-H_{298}) (KJ/mol)		S (J/mol K)	(H-H_{298}) (KJ/mol)
298.15	107.601	0.000		110.039	0.000
300	107.931	0.099		110.352	0.094
400	122.161	5.046		125.055	5.207
500	133.236	10.009		136.712	10.433
600	142.301	14.981		146.442	15.772
700	149.973	19.958		154.843	21.223
800	156.622	24.938		162.270	26.786
900	162.489	29.919		168.955	32.463
1000	167.740	34.902		175.053	38.251
1100	172.490	39.886		180.676	44.153
1197	176.703	44.722		185.756	49.985

4. Conclusions

To summarize, the dynamical and thermodynamic properties of PbX (X = S, Se, Te) using density functional theory and linear response theory are performed. We obtain the phonon frequencies at the Brillouin zone center (Γ point), as well as X and L points, and the phonon dispersion curves, as well as corresponding phonon density of states. The calculated phonon frequencies are in reasonable agreement with experimental data and other similar theoretical calculations. The thermodynamic properties including the phonon contribution to the Helmholtz free energy ΔF, the phonon contribution to the internal energy ΔE, the entropy S, and the constant-volume specific heat C_v are determined within the harmonic approximation based on the calculated phonon density of states. If 298 K is taken as a reference temperature, the values of H-H_{298} have been calculated and compared with the available experimental data.

Acknowledgments

This work was supported by National Natural Science Foundation of China (No. 12004055, 11904037).

References

[1] L.D. Hicks, T.C. Harman, X. Sun, M.S. Dresselhaus, Phys. Rev. B 53, R10493 (1996); https://doi.org/10.1103/PhysRevB.53.R10493

[2] T.C. Harman, P.J. Taylor, M.P. Walsh, B.E. Laforge, Science 297, 2229 (2002); https://doi.org/10.1126/science.1072886

[3] M.S. Dresselhaus, G. Chen, M.Y. Tang, R. Yang, H. Lee, D. Wang, Z. Ren, J.-P. Fleurial, P. Gogna, Adv. Mater. 19, 1043 (2007); https://doi.org/10.1002/adma.200600527

[4] H. Preier, Appl. Phys. 20, 189 (1979); https://doi.org/10.1007/BF00886018

[5] S. Chatterjee, U. Pal, Opt. Eng. 32, 2923 (1993); https://doi.org/10.1117/12.148123

[6] K.D. Dobson, G. Hodes, Y. Mastai, Sol. Energy Mater. Sol. Cells 80, 283 (2003); https://doi.org/10.1016/j.solmat.2003.06.007

[7] N.K. Mudugamuwa, D.M.N.M. Dissanayake, A.A.D.T. Adikaari, S.R.P. Silva, Sol. Energy Mater. Sol. Cells 93, 549 (2009); https://doi.org/10.1016/j.solmat.2008.11.039

[8] M. Lach-hab, D.A. Papaconstantopoulos, M.J. Mehl, J. Phys. Chem. Solids 63, 833 (2002); https://doi.org/10.1016/S0022-3697(01)00237-2

[9] Z. Nabi, B. Abbar, S. Mecabil, A. Khalfi, N. Amrane, Comp. Mater. Sci. 18, 127 (2000); https://doi.org/10.1016/S0927-0256(99)00099-3

[10] A. Svane, N.E. Christensen, M. Cardona, A.N. Chantis, M. van Schilfgaarde, T. Kotani, Phys. Rev. B 81, 245120 (2010); https://doi.org/10.1103/PhysRevB.81.245120

[11] M.M. Elcombe, Proc. R. Soc. London, Ser. A 300, 210 (1967); https://doi.org/10.1098/rspa.1967.0166

[12] W. Cochran, R.A. Cowley, G. Dolling, M.M. Elcombe, Proc. R. Soc. London, Ser. A 293, 433 (1966).

[13] P.R. Vijayraghavan, S.K. Sinha, P.K. Iyengar, Proc. Nucl. Phys. Solid State Phys. (India) 16C, 208 (1973).

[14] M. Cardona, R.K. Kremer, R. Lauck, G. Siegle, J. Serrano, A.H. Romero, Phys. Rev. B 76, 075211 (2007); https://doi.org/10.1103/PhysRevB.76.075211

[15] J. An, A. Subedi, D.J. Singh, Solid State Commun. 148, 417 (2008); https://doi.org/10.1016/j.ssc.2008.09.027

[16] A.H. Romero, M. Cardona, R.K. Kremer, R. Lauck, G. Siegle, J. Serrano, X.C. Gonze, Phys. Rev. B 78, 224302 (2008).

[17] Y. Zhang, X.Z. Ke, C.F. Chen, J. Yang, P.R.C. Kent, Phys. Rev. B 80, 024304 (2009); https://doi.org/10.1103/PhysRevB.80.024304

[18] O. Kilian, G. Allan, L. Wirtz, Phys. Rev. B 80, 245208 (2009); https://doi.org/10.1103/PhysRevB.80.245208

[19] Y. Bencherif, A. Boukra, A. Zaoui, M. Ferhat, Infrared Phys. Technol. 54, 39 (2011); https://doi.org/10.1016/j.infrared.2010.11.001

[20] S. Baroni, P. Giannozzi, A. Testa, Phys. Rev. Lett. 58, 1861 (1987); https://doi.org/10.1103/PhysRevLett.58.1861

[21] S. Baroni S. de Gironcoli, A. Dal Corso, P. Giannozzi, Rev. Mod. Phys. 73, 515 (2001); https://doi.org/10.1103/RevModPhys.73.515

[22] A. Kuwabara, T. Tohei, T. Yamamoto, I. Tanaka, Phys. Rev. B 71, 064301 (2005); https://doi.org/10.1103/PhysRevB.71.064301

[23] T. Tohei, A. Kuwabara, F. Oba, I. Tanaka, Phys. Rev. B 73, 064304 (2006); https://doi.org/10.1103/PhysRevB.73.064304

[24] R.O. Jones, O. Gunnarsson, Rev. Mod. Phys. 61, 689 (1989); https://doi.org/10.1103/RevModPhys.61.689

[25] P. Hohenberg, W. Kohn, Phys. Rev. 136, B864 (1964); https://doi.org/10.1103/PhysRev.136.B864

[26] P.E. Blöchl, Phys. Rev. B 50, 17953 (1994); https://doi.org/10.1103/PhysRevB.50.17953

[27] X. Gonze, J.-M. Beuken, R. Caracas, F. Detraux, M. Fuchs, G.-M. Rignanese, L. Sindic, M. Verstraete, G. Zerah, F. Jollet, M. Torrent, A. Roy, M. Mikami, P. Ghosez, J.-Y. Raty and D.C. Allan, Comput. Mater. Sci. 25, 478 (2002); https://doi.org/10.1016/S0927-0256(02)00325-7

[28] The ABINIT code is a common project of the Universite Catholique de Louvain, Corning Incorporated, and other contributors (URL http://www.abinit.org).

[29] S.Y. Savrasov, Phys. Rev. B 54, 16470 (1996); https://doi.org/10.1103/PhysRevB.54.16470

[30] S.H. Wei, A. Zunger, Phys. Rev. B 55, 13605 (1997); https://doi.org/10.1103/PhysRevB.55.13605

[31] R. Dalven, Infrared Phys. 9, 141 (1969); https://doi.org/10.1016/0020-0891(69)90022-0

[32] O. Madelung, M. Schulz, H. Weiss, Numerical Date and Functional Relationships in Science and Technology, Landolt-Bornstei, New Series, Vol. 17, Springer, Berlin, 1983.

[33] M.A. Omar, Elementary Solid State Physics: Principles and Applications, Addison-Wesley Publishing Company, Reading, Massachusetts, 1975.

[34] C. Lee, X. Gonze, Phys. Rev. B 51, 8610 (1995); https://doi.org/10.1103/PhysRevB.51.8610

[35] I. Barin, Thermochemical Data of Pure Substances, 3rd ed. VCH, New York, 1995; https://doi.org/10.1002/9783527619825